Vibrationally resolved N 1s absorption spectra of the acrylonitrile molecule

Ilakovac, Vita; Houari, Ymene; Carniato, Stephane; Gallet, Jean-Jacques; Kukk, Edwin; Horvatić, Davor

Source / Izvornik: **Physical Review A, 2012, 85**

Journal article, Published version
Rad u časopisu, Objavljena verzija rada (izdavačev PDF)

https://doi.org/10.1103/PhysRevA.85.062521

Permanent link / Trajna poveznica: https://urn.nsk.hr/urn:nbn:hr:217:253815

Vibrationally resolved N 1*s* absorption spectra of the acrylonitrile molecule

Vita Ilakovac,[1,2,*] Ymène Houari,[1] Stéphane Carniato,[1] Jean-Jacques Gallet,[1] Edwin Kukk,[3] and Davor Horvatić[4]

[1]*Laboratoire de Chimie Physique–Matière et Rayonnement, Université Pierre et Marie Curie, CNRS UMR 7614, F-75231 Paris, France*

[2]*Université de Cergy-Pontoise, F-95031 Cergy-Pontoise, France*

[3]*Department of Physics, University of Turku, FI-20014 Turku, Finland*

[4]*Department of Physics, University of Zagreb, Bijenička c.32, P.O. Box 162, 10001 Zagreb, Croatia*

(Received 26 April 2012; published 29 June 2012)

Besides two strong $\pi^*_{\perp 1}$ and $\pi^*_{\parallel}$ resonances in the 398- to 400-eV energy range, N 1*s* near edge x-ray absorption fine structure spectra of acrylonitrile molecules have a less intense 401- to 403-eV doublet. The two components correspond to the N $1s \rightarrow \pi^*_{\perp 2}$ and N $1s \rightarrow D^*_{\parallel}$ transitions, where $D^*_{\parallel}$ is a diffuse state with strong Rydberg character. The vibrational analysis shows that in the $D^*_{\parallel}$ excited state, two low-energy *out-of-plane* normal modes are strongly excited. The $\pi^*_{\perp 2}$ excitation triggers a set of *in-plane* vibrations, in particular, two C=C–C≡N bendings of the molecule.

DOI: 10.1103/PhysRevA.85.062521 PACS number(s): 33.20.Rm, 31.15.E−, 33.20.Tp, 33.70.Ca

I. INTRODUCTION

To understand how an organic molecule reacts with its environment one needs to know its structure and the way it moves. Vibrational dynamics drives and controls its interactions with other molecules and surfaces. Different spectra of vibrational modes can be excited depending on the quantum of energy and the way this energy is transferred to the molecule. Stretching vibrational modes can easily be observed in spectra of core-excited molecules, particularly if they are linear or centro-symmetric [1–4]. Their energy quanta of few hundreds of meV are usually larger than the mean lifetime broadening of a core-hole excitation of light elements (≈100 meV). Thus they can easily be resolved in the absorption spectra of the gas phase using high-resolution synchrotron light sources. For more complex molecules, a tendency to change angles introduces bending [5–8], and torsional degrees of freedom [9,10]. Characterized by small energy spacing of few *tens* of meV or even less, these vibrational excitations cannot be resolved despite the high experimental resolution. However, low-frequency modes are particularly interesting as they can be excited by thermal fluctuations and thus contribute to reaction activation. Nitrile molecules, for example, frequently bend their C-C≡N linear part in order to attach to silicon surfaces [11–14].

Acrylonitrile (see Fig. 1) is a model molecule for vibrations accompanying core-hole excitations, because it is one of the smallest molecules with many vibrational modes of different character. Among its 15 vibrational modes, six of them are stretchings, three are bendings, one is torsion, and others are of wagging, rocking, and deformation character [15,16]. Accommodating a core electron in the lowest unoccupied $\pi^*_{\perp 1}$ state triggers a large set of in-plane normal modes, while $\pi^*_{\parallel}$ excitation produces bending vibrations combined with C≡N stretching [17]. This work reports a state-of-the-art vibrational analysis of higher energy excited states, close to the ionization potential, in the energy region where the valence states already have a strong Rydberg character.

The article is organized as follows: Details of the calculations of the vibrational progression are presented in Sec. II (for experimental details see Ref. [17]). Experimental and calculation results are compared and discussed in Sec. III.

II. CALCULATIONS

The calculation of the vibrational progression is performed in the Franck-Condon approximation. The intensity and the energy of the transition from the initial $(n_1,n_2,\ldots)$ to the final vibrational state $(n'_1,n'_2,\ldots)$ are calculated as

$$I(n_1 \rightarrow n'_1, n_2 \rightarrow n'_2, \ldots) = \prod_{m=1}^{\mathcal{M}} \left|\left\langle \psi'_{n'_m} \middle| \psi_{n_m} \right\rangle\right|^2,$$
$$E(n_1 \rightarrow n'_1, n_2 \rightarrow n'_2, \ldots) = \sum_{m=1}^{\mathcal{M}} [E(n'_m) - E(n_m)], \quad (1)$$

where n_m and n'_m are the quantum vibrational numbers of the mode m in the initial and excited state, respectively.

For a molecule with N atoms, FC amplitudes,

$$FC(n_m \rightarrow n'_m) = \left\langle \psi'_{n'_m} \middle| \psi_{n_m} \right\rangle, \quad (2)$$

are calculated directly for $\mathcal{M} = 3N - 6$ vibrational modes, as overlaps between the ground-state (ψ_{n_m}) and excited-state $(\psi'_{n'_m})$ wave functions, which are themselves solutions of the Schrödinger equation for a mode m:

$$\frac{\partial^2 \psi_{n_m}}{\partial q_m^2} + V_m(q_m)\psi_{n_m} = E_{n_m}\psi_{n_m}. \quad (3)$$

Here q_m represents displacement from the ground-state geometry (labeled by $q = 0$) in the direction of the ground-state normal coordinate of the mode m, and $V_m(q_m)$ is the corresponding potential. For a more detailed explanation of the model see Ref. [17].

The calculations were done using the density functional theory with Becke three-parameter hybrid exchange [18] and the Lee-Yang-Parr gradient-corrected correlation functional [19] (B3LYP) implemented in the GAMESS(US) program [20]. An accurate, IGLOO-III basis set [21] completed by *sp* and *d* diffuse Gaussians is used for the nitrogen and carbon atoms in order

*vita.ilakovac-casses@upmc.fr

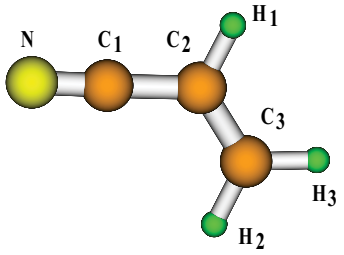

FIG. 1. (Color online) N≡C−CH=CH_2, acrylonitrile molecule.

to simulate valence states with a strong admixture of Rydberg character. The 6-311G** basis set [22] is used for hydrogen atoms. The core-excitation energies are computed for a triplet final state using the ΔKohn-Sham (ΔKS) approach. The relativistic correction of 0.3 eV for nitrogen [23] has been included. The singlet-triplet correction calculated by the sum method of Ziegler *et al.* [24] was included in the final calculation of potential curves. Transition moments corresponding to N 1*s* excitation energies were computed at a configuration interaction post Hartree-Fock (CI) level of theory, including single and double excitations. The Schrödinger equation in normal coordinates is resolved numerically by the finite difference method.

III. RESULTS AND DISCUSSION

A. Calculation of the ground and excited states

In the electronic ground state, the acrylonitrile is a planar noncentrosymmetric molecule, belonging to symmetry point group C_S (see Fig. 1). The calculated interatomic distances and angles are compared to experimental values [25,26] in Table I. They differ by less than 1.3%.

The electronic ground-state configuration of its 20 valence electrons has been determined using photoelectron spectroscopy [27]. For the outermost valence molecular orbitals *perpendicular* to the plane of the molecule, the π states are delocalized along the C=C–C≡N chain due to conjugative interaction between the C=C bond and the C≡N bond. This conjugation gives rise to two bonding, $1a''$, $2a''$, and two antibonding, $3a''$, $4a''$ orbitals. The π states which lie *in* the molecular plane are mostly localized on the C≡N group. They lead to one bonding orbital, $12a'$ and one antibonding orbital, $13a'$ (LUMO + 1), whose energy is not affected by conjugation effects.

TABLE I. Experimental and calculated interatomic distances and angles of the acrylonitrile molecule in its electronic ground state.

Distances (Å)	Expt. [25]	Expt. [26]	Calculation
$N{\equiv}C_1$	1.164	1.167	1.152
$C_1{-}C_2$	1.426	1.438	1.428
$C_2{=}C_3$	1.339	1.343	1.331
C-H	1.086	1.130	1.082
Angles (°)			
$C_1C_2C_3$	122.6	121.7	123.0
$C_2C_3H_2$	121.7	120	121.6
NC_1C_2		178	178.6

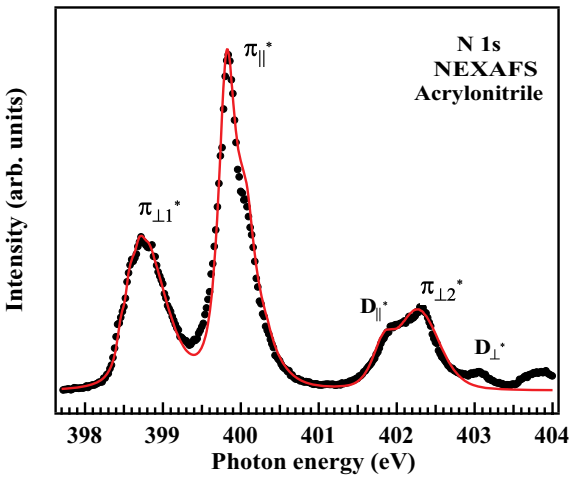

FIG. 2. (Color online) The entire experimental N 1*s* NEXAFS spectrum (black points) of the acrylonitrile molecule compared to calculations including vibrational analysis (red line). The spectra show two strong low-energy structures ($\pi^*_{\perp 1}$ and $\pi^*_{\parallel}$), a $D^*_{\parallel}$–$\pi^*_{\perp 2}$ doublet and a small $D^*_{\perp}$ structure close to the ionization potential. Experimental details are given in Ref. [17].

The N 1*s* NEXAFS spectrum of acrylonitrile (see Fig. 2) is essentially dominated by two strong peaks in the low-energy part of the spectrum [17,28,29]. The lowest band is assigned to an out-of-plane N $1s \rightarrow \pi^*_{\perp 1}$(C=C–C≡N) ($3a''$) transition and the second and most intense to an in-plane N $1s \rightarrow \pi^*_{\parallel}$(C≡N) ($13a'$) transition. The next structure is usually attributed to a transition to the second $\pi^*_{\perp 2}$(C=C–C≡N) ($4a''$) unoccupied orbital [28,29]. Our high-resolution experimental spectrum clearly shows that the third structure has two components. A polarization dependent NEXAFS study on acrylonitrile adsorbed on Pt and Au surfaces [29] shows that the two components of the doublet cannot have the same symmetry (a'') as they do not have the same polarization behavior. The present work shows that the second component of the doublet corresponds to a transition to a valence-Rydberg mixed state of a' symmetry ($D^*_{\parallel}$).

In order to identify the two components of the doublet we performed calculation of direct ΔKS excited state energies (i.e., the energy difference between the ground state and the excited state without changing the molecular geometry). Table II shows energies of the first excited states dependent on the Gaussian basis used for N and C atoms. Using the IGLOO-III for N and the 6-311G** for C (B_1) gives two low-energy features, corresponding to the excitation to $\pi^*_{\perp 1}$ at 398.44 eV and to $\pi^*_{\parallel}$ at 399.30 eV, and the third excited state at 402.62 eV, of the a'' symmetry ($\pi^*_{\perp 2}$). The next higher excitation energies exceeded 403 eV. Defining the IGLOO-III basis for the C atom (B_2) includes another a'' ($D^*_{\perp}$) state below the ionization potential (IP = 405.4 eV). Its energy of 404.60 eV is, however, too high compared to the experimental values. Extending the IGLOO-III basis set by *sp*-diffuse Gaussians on the N atom (B_3) decreases the excitation energy of an a' state [$D^*_{\parallel}$; Fig. 3(a)] state below the $\pi^*_{\perp 2}$ resonance. Finally, including additional *sp* and *d* diffuse Gaussians on N and C atoms (B_4) gives a set of first excitation energies which perfectly match experimental data in the 400- to 403-eV

TABLE II. ΔKS excited-state energies of acrylonitrile calculated using different Gaussian basis set for N and C atoms: B_1 (IGLOO-III on N and 6-311** on C), B_2 (IGLOO-III on N and C), B_3 (IGLOO-III + diffuse *sp* on N and IGLOO-III on C), B_4 (IGLOO-III + diffuse *sp*-*d* on N and C). Diffuse orbitals $D^*_\perp$ and $D^*_\parallel$ appear in the region of interest only when a more complete basis than IGLOO-III is used. At the same time, the localized states merge in energy. The last two columns are dedicated to excitation energies calculated at the CI level of theory (CI-en.) and corresponding relative transition moments (CI-mom., in arb. units). First CI energy is shifted in order to match the first ΔKS energy. IP is for ionization potential.

Basis		ΔKS (eV) B_1	ΔKS (eV) B_2	ΔKS (eV) B_3	ΔKS (eV) B_4	CI-en (eV) B_4	CI-mom. (rel.) B_4
Orb.	Sym.						
a''	$(\pi^*_{\perp 1})$	398.44	398.40	398.40	398.40	398.40	65
a'	$(\pi^*_\parallel)$	399.30	399.26	399.25	399.25	399.25	100
a'	$(D^*_\parallel)$	–	–	402.07	401.90	402.14	3
a''	$(\pi^*_{\perp 2})$	402.62	402.37	402.37	402.26	402.50	35
a''	$(D^*_\perp)$	–	404.60	403.66	403.06	404.40	3
IP					405.40		

window, namely, $E(D^*_\parallel) = 401.90$ eV, $E(\pi^*_{\perp 2}) = 402.26$ eV, and $E(D^*_\perp) = 403.06$ eV. Similar states, with strong valence-Rydberg admixture, are observed in N 1*s* excited pyridine [30].

The form of the two molecular orbitals of the doublet, $D^*_\parallel$ and $\pi^*_{\perp 2}$, is shown in Fig. 3. Left side panels [(a) and (c)] present ground-state forms of $D^*_\parallel$ and $\pi^*_{\perp 2}$ molecular orbitals while right hand panels [(b) and (d)] show corresponding excited-state changes. In the ground state, both orbitals are spread on the N≡C–C part of the molecule. The orbital weight on the N and C_1 atoms is similar. The in-plane $D^*_\parallel$ orbital has poorer density on the H–C=C–H_2 part of the molecule. In the respective excited states the density is much more spread over the whole molecule. In the case of the $\pi^*_{\perp 2}$ accommodating a supplementary electron, the proximity of the N atom is slightly depleted. On the other hand, when the electron is excited in the $D^*_\parallel$ state, a large electronic density is localized around the C_1 atom.

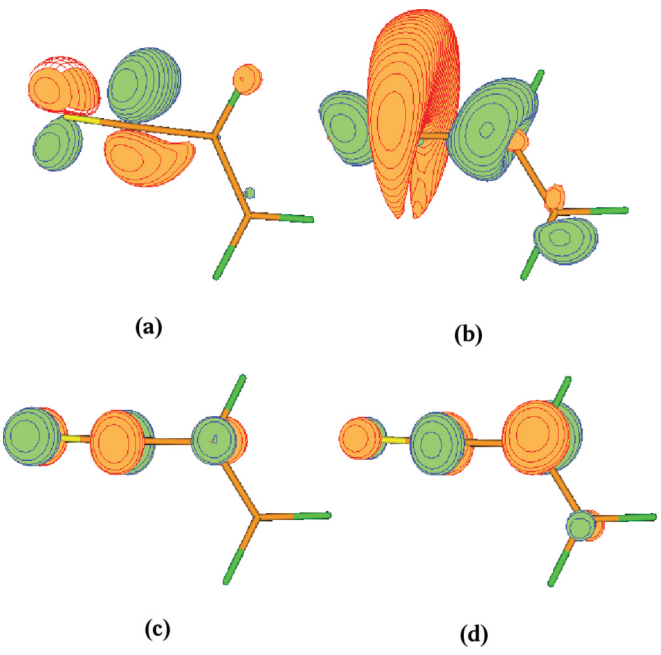

FIG. 3. (Color online) Ground [(a) and (c)] and excited [(b) and (d)] state forms of $D^*_\parallel$ and $\pi^*_{\perp 2}$ orbitals. The $D^*_\parallel$ orbital changes strongly in the excited state: The small bag close to the C_1 atom in the ground state (a) surrounds the C_1 atom like a crescent moon in the excited state (b). On the other hand, the $\pi^*_{\perp 2}$ orbital changes much less when accommodating the supplementary electron [(c) and (d)]: There is a slight transfer of one part of the N states to the H–C=C–H_2 part of the molecule.

The calculation of the N 1*s* excitation energies and transition moments was performed at the *ab initio* CI level of theory. They were extended high enough to include a description of the full spectrum until the IP. Two separated CI calculations using different active subspaces including a' and a'' states were considered. For both CI spaces, the considered orbitals were obtained from a unique general valence bond (GVB) computation of the lowest core-excited state of a'' symmetry. This state was variationally determined by fixing the occupation of the core spin orbital to zero and placing the excited electron in the lowest unoccupied orbitals π^* with selected symmetry (a''). Each active subspace was limited to the singly occupied N 1*s* inner shell, the 10 highest doubly occupied valence orbitals and the 70 lowest unoccupied valence-Rydberg virtual orbitals. The transition moments were computed in the dipole-length form. Energies of the transitions N $1s \rightarrow \pi^*_{\perp 1}$ (a'' subspace) and N $1s \rightarrow \pi^*_\parallel$ (a' subspace) are shifted in order to match the corresponding ΔKS values.

Both ΔKS (see Table II) and post-HF CI calculations give the same energy order and symmetries of the first excited states of acrylonitrile. In particular, the 401- to 403-eV doublet is composed of an a' state at lower energy and an a'' state at higher energy. Moreover, the a' state has a lower transition moment compared to the a'' state, which perfectly matches experimental data.

B. Calculation of vibrational progressions

1. Ground-state normal modes

Acrylonitrile has 15 normal vibrational degrees of freedom [15,16]. Eleven vibrations are in the plane of the molecule (A'), and four are out-of-plane, belonging to the A'' irreducible representation. The corresponding calculated ground-state wave numbers (σ in cm^{-1}) and energies ($\hbar\omega$ in eV) are compared to experimental values [16] in Table III. The experimental values for modes $m = 13,14,15$ are given only for the liquid phase. Wave numbers of a particular mode m are calculated from the first vibrational quanta $h\nu = E_1 - E_0$, where E_0 and E_1 are the first two eigenvalues of the corresponding potential. The calculated values correspond well to experimental data. For the modes with the wave number (σ) greater than 1000 cm^{-1}, the calculated value is only 1%–3% higher, while for those with smaller σ, it is less than 4%–8% higher. The probability of thermal excitation to the $n = 1$ vibrational state at room temperature is less than 30% (case of the C–C≡N *in-plane* bending). In the following we will thus consider that $n = 0$ for all normal modes in the ground state.

TABLE III. Vibrational modes in the ground state, and $\pi^*_\perp$ and D^* excited states. First two columns are as follows: number (m), symmetry, and nature of the vibrational mode. s, d, r, b, w, t, are for stretching, deformation, rocking, bending, wagging, and torsion. Ground state as follows: experimental (σ_{expt}, Ref. [16], [l]Liq. phase), calculated (σ) wave number in cm^{-1}, and $\hbar\omega = E_1$-E_0 in meV. $\pi^*_\perp$ and $D^*_\parallel$ excited states as follows: E_1-E_0 in meV and the first FC factors for each mode. *Out-of-plane* modes' potentials have either symmetric simple well or symmetric double well (indicated by sdw) form. Their vibrational quanta are expressed in E_2-E_0 as the FC factors of odd wave functions is equal to zero. Only even FC factors are indicated in the case of $D^*_\parallel$ *out-of-plane* modes for the sake of brevity.

		Ground state			$D^*_\parallel$ excited state							$\pi^*_{\perp 2}$ excited state				
m	Character	σ_{expt}	σ	$\hbar\omega$	E_1-E_0		FC(0)	FC(1)	FC(2)	FC(3)		E_1-E_0		FC(0)	FC(1)	FC(2)
A'	In-plane															
1	C-H s	3125	3241	400	399		**1.00**	0.00	0.00	0.00		409		**1.00**	0.00	0.00
2	C-H s	3078	3159	390	382		**1.00**	0.00	0.00	0.00		400		**0.99**	0.01	0.00
3	C-H s	3042	3145	389	391		**1.00**	0.00	0.00	0.00		394		**1.00**	0.00	0.00
4	C≡N s	2239	2323	287	282		**0.92**	0.08	0.00	0.00		286		**1.00**	0.00	0.00
5	C=C s	1615	1671	206	199		**1.00**	0.00	0.00	0.00		212		**0.89**	0.09	0.02
6	CH_2 d	1416	1439	178	173		**0.97**	0.03	0.00	0.00		182		**1.00**	0.00	0.00
7	CH r	1282	1320	163	158		**1.00**	0.00	0.00	0.00		165		**0.65**	0.28	0.06
8	CH_2 r	1096	1119	138	135		**0.95**	0.05	0.00	0.00		137		**0.67**	0.27	0.05
11	C–C s	869	879	109	107		**0.99**	0.00	0.01	0.00		114		**0.39**	0.37	0.18
13	C=C–C b	570[l]	574	71	106		**0.94**	0.03	0.02	0.00		68		0.29	**0.41**	0.23
15	C–C≡N b	242[l]	236	29	59		**0.63**	0.21	0.11	0.04		35		0.20	**0.50**	0.30
					E_2-E_0		FC(0)	FC(2)	FC(4)	FC(6)	FC(8)	E_2-E_0		FC(0)	FC(1)	FC(2)
A''	Out-of-plane															
9	CH_2=CH w	972	1005	124	224		**1 00**	0.00	0.00	0.00	0.00	122	sdw	**0.99**	0.00	0.00
10	CH_2=C w	954	987	122	271		**1.00**	0.00	0.00	0.00	0.00	185		**0.98**	0.00	0.02
12	C=C t	683	706	87	76	sdw	0.120	**0.51**	0.33	0.04	0.00	198		**1.00**	0.00	0.00
14	C–C≡N b	362[l]	343	42	99	sdw	0.01	0.07	0.20	**0.38**	0.30	166		**0.97**	0.00	0.03

The vibrational progression of the first two resonances in the NEXAFS spectrum ($\pi^*_{\perp 1}$ at 398.7 eV and $\pi^*_\parallel$ at 399.8 eV) has been already extensively discussed [17]. In the following, we present the results of the calculations of the 401.5- to 402.5-eV doublet. The small structure at ≈403 eV is not discussed in the present paper.

2. Transition to the $D^*_\parallel$ excited state

When an N 1s electron is excited to the $D^*_\parallel$ unoccupied state, *in-plane* normal modes with $\hbar\omega > 100$ meV ($\sigma > 1000$ cm^{-1}) do not change drastically. In the excited state their potentials have the form of a simple well, as in the ground state, and their vibrational quanta are close to the ground state value (see Table III). The only mode which is relatively excited is the C–C≡N *in-plane* bending mode ($m = 15$). Its vibrational quantum increases from ≈30 meV in the ground state to ≈60 meV in the excited state. The Franck-Condon factor for $n' = 1$, FC(1) = 21%, is important, but is still much lower than the probability of the $n = 0$ to $n' = 0$ transition, namely 63%.

Out-of-plane normal modes of high energy quanta, CH_2=CH and CH_2=C waggings (m = 9,10) do not change the vibrational state with electronic excitation. On the other hand, low energy *out-of-plane* modes, C=C torsion ($m = 12$) and the C–C≡N bending ($m = 14$), with symmetric double well potentials in the excited state, are highly excited. In the ground state, these modes have potentials of a symmetric simple well form. Thus the overlap of the ground state $n = 0$ with all the odd functions of the excited state $m = 12$ and $m = 14$ potentials are zero. This is the reason why the value of the energy difference E_2-E_0 replaces the quantum of these excitations in Table III. The coupling with the first even levels of these potentials is weak because the amplitude of the excited-state wave functions is negligible in the range where the ground-state wave function is important. Franck-Condon factors increase when the eigenvalue of the excited state potential approaches the maximum of the barrier (i.e., when the two wells communicate due to the tunneling effect). Thus for the $m = 14$ mode the transition to the $n_{14} = 6$ is the highest (see Fig. 4). On the other hand, the extremely low value of the Franck-Condon factor of $n_{14} = 0$ decreases the probability of the all-mode vibrational fundamental. Its energy is chosen to be the lowest E'_{m0}-E_{m0} difference, where E'_{m0} (E_{m0}) corresponds to the vibrational fundamental of the mode m in the excited (ground) state. In the case of the excitation to the $D^*_\parallel$ state the minimal value of the E'_{m0}-E_{m0} difference is for $m = 14$ and equals 401.4 eV. Important excitation of the $m = 14$ and 12 modes pushes the maximum of the vibrational progression to 420 meV higher energy. The most probable vibrational excitation, the highest vertical bar in Fig. 6 is the m = 14,12–bimodal excitation with $n_{14} = 6$ and $n_{12} = 2$.

3. Transition to the $\pi^*_{\perp 2}$ excited state

In the $\pi^*_{\perp 2}$ excited state, only one *out-of-plane* normal mode, CH_2=CH wagging ($m = 9$), potential form changes in the excited state to a symmetric double well (see Table III). This decreases its frequency by a factor of 2 (remark that the E_2-E_0 is given for the excited state of *out-of-plane* normal modes, like in the case of the $D^*_\parallel$ excited state). The vibrational quanta of the other three *out-of-plane* modes

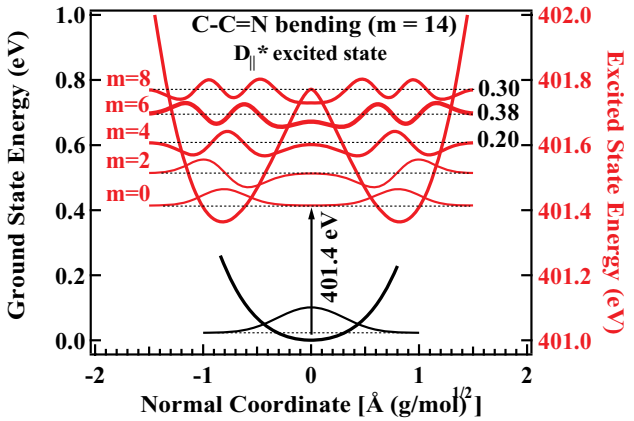

FIG. 4. (Color online) Ground state (black solid line), $D_{\|}^{*}$ excited state (orange) potential surface of its most excited, C–C≡N out-of-plane bending vibrational mode ($m = 14$). Corresponding wave functions (solid lines) and eigenvalues (dashed lines) are drawn for each potential. The arrow indicates a vertical transition (at $q = 0$) between ψ_0 and ψ_0'. The probability of the excitation of the three most important quantum states is indicated at the right side of the excited potential.

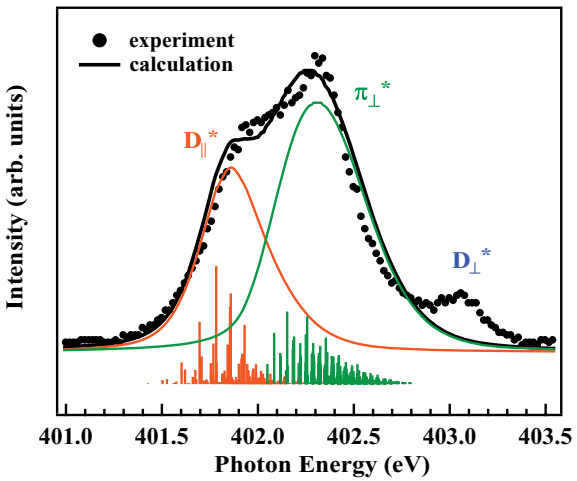

FIG. 6. (Color online) Calculation of the 401.5- to 402.5-eV doublet compared to the experiment. It is composed of vibrational progressions of the $D_{\|}^{*}$ excited state (orange line, maximum at 401.9 eV) and the $\pi_{\perp 2}^{*}$ excited state (green line, centered at 402.35 eV). Addition of these two structures (black line) matches experimental spectra well.

is either decreased ($m = 10$), or increased ($m = 12,14$). Despite these modifications, *out-of-plane* modes are poorly vibrationally excited.

The *in-plane* normal mode potentials in the $\pi_{\perp 2}^{*}$ excited state conserve the simple well form, as in the $D_{\|}^{*}$ excited state. Table III shows that the vibrational quanta are less than 5% apart from these in the ground state, except for C–C≡N bending, where this difference is ≈20%. The potential minima are however more or less shifted compared to the ground-state potential. The potential shift and the slight frequency modification for modes with $\hbar\omega < 180$ meV, like CH and CH_2 rocking ($m = 7,8$), C–C stretching ($m = 11$), and C=C–C (see Fig. 5) and C–C≡N bendings ($m = 13, 15$) induce a high probability of the excitation to their $n' = 1$ level. The vibrational population of the lowest frequency C=C–C and C–C≡N bending modes is even reversed [i.e., the probability of the $n' = 1$ vibrational state is larger than the probability of the vibrational fundamental (41% and 50%, for $m = 13, 15$, respectively]. The most probable vibrational excitation corresponds to the $m = 13,15$–bimodal transition to $n'_{13} = 1$ and $n'_{15} = 1$. The low Franck-Condon factors for $n' = 0$ of almost half of the *in-plane* normal modes decrease the probability of the all-mode vibrational fundamental. The minimal value of the E'_{m0}-E_{m0} difference for the $\pi_{\perp 2}^{*}$ excited state is 402 eV (for $m = 13$). Excitation of the modes $m = 7, 8, 11, 13$, and 15 shifts the maximum of the vibrational progression to 320 meV higher energy.

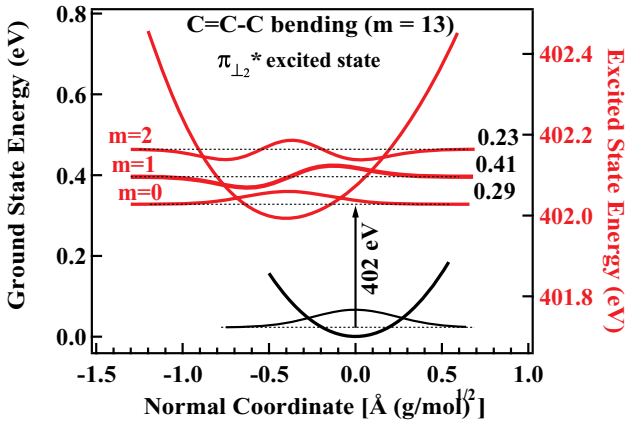

FIG. 5. (Color online) Ground state (black), $\pi_{\perp}^{*}$ excited state (orange) potential surface projected to its second most excited, out-of-plane C=C–C bending vibrational mode ($m = 13$). Wave functions and eigenvalues are indicated. The probability of the excitation to the three states with most important Franck-Condon factors is indicated at the right side of the excited potential.

IV. CONCLUSION

Vibrationally resolved NEXAFS N 1*s* spectra of the acrylonitrile molecule have been calculated in the energy range from 401 to 404 eV, where two close resonances form a not clearly resolved doublet. This study completes previous calculation of the onset of the NEXAFS N 1*s* spectra (i.e., absorption to the $\pi_{\perp 1}^{*}$ and $\pi_{\|}^{*}$ states) at 398.7 and 399.8 eV, respectively [17]. The first component of the higher energy doublet corresponds to the accommodation of the N 1*s* electron in the $D_{\|}^{*}$ unoccupied diffuse state. It appears below the ionization potential only if an extended IGLOO-III Gaussian basis set, including diffuse *sp* and *d* states is used on N and C atoms. The need for the diffuse Gaussians augmented basis set points to the fact that this valence state has an important admixture of Rydberg character. The second component, at only 420 meV higher energy corresponds to the N 1*s* → $\pi_{\perp 2}^{*}$ (C=C–C≡N) transition. Transition to the $D_{\|}^{*}$ diffuse state produces molecular motion which concerns mostly C=C torsion and C–C≡N *out-of-plane* bending, while the transition to the $\pi_{\perp 2}^{*}$ triggers mostly *in-plane* C=C–C and C–C≡N bendings. The perfect agreement of the entire

experimental N 1*s* NEXAFS spectra and the calculation including vibrational analysis is shown in Fig. 6.

It is interesting to remark that when the N 1*s* electron is accommodated in the $D^*_{\parallel}$ orbital, which is *symmetric* relative to the molecular plane, low-energy *out-of-plane* normal modes are strongly excited, while the *in-plane* modes tend to conserve the same vibrational state. On the other hand, when the N 1*s* electron is accommodated in the $\pi^*_{\perp 2}$ molecular orbital, which is *asymmetric* relative to the molecular plane, five *in-plane* normal modes are strongly excited. The *out-of-plane* modes here tend to stay in the same vibrational state. Similar enhancement of the *in-plane* normal modes has already been observed for the excitation to the molecular-plane-*asymmetric* $\pi^*_{\perp 1}$ orbital [17]. On the contrary, in the case of N 1*s* $\rightarrow$ $\pi^*_{\parallel}$ transition the most excited vibrational modes are *in-plane* vibrations.

ACKNOWLEDGMENTS

The experimental work was supported by the EC Access to Research Infrastructures program. The authors also thank the staff of the MAX-lab for technical support and M. Huttula, R. Sankari, and J. Nikkinen for help with the experiment.

[1] S. J. Osborne *et al.*, J. Chem. Phys. **106**, 1661 (1997).
[2] T. D. Thomas, L. J. Saethre, S. L. Sorensen, and S. Svenson, J. Chem. Phys. **109**, 1041 (1998).
[3] S. Sundin, L. J. Saethre, S. L. Sorensen, A. Ausmees, and S. Svensson, J. Chem. Phys. **110**, 5806 (1999).
[4] T. X. Carroll, K. J. Borve, L. J. Saethre, J. D. Bozek, E. Kukk, J. A. Hahne, and T. D. Thomas, J. Chem. Phys. **116**, 10221 (2002).
[5] E. Kukk, J. D. Bozek, and N. Berrah, Phys. Rev. A **62**, 032708 (2000).
[6] S. Carniato, V. Ilakovac, J.-J. Gallet, E. Kukk, and Y. Luo, Phys. Rev. A **70**, 032510 (2004).
[7] S. Carniato, V. Ilakovac, J.-J. Gallet, E. Kukk, and Y. Luo, Phys. Rev. A **71**, 022511 (2005).
[8] M. Alagia, M. Lavollée, R. Richter, U. Ekström, V. Carravetta, D. Stranges, B. Brunetti, and S. Stranges, Phys. Rev. A **76**, 022509 (2007).
[9] M. Abu-samha, K. J. Børve, L. J. Saethre, and T. D. Thomas, Phys. Rev. Lett. **95**, 103002 (2005).
[10] M. Abu-samha and K. J. Børve, Phys. Rev. A **74**, 042508 (2006).
[11] F. Tao, W. S. Sim, G. Q. Xu, and M. H. Qiao, J. Am. Chem. Soc. **123**, 9397 (2001).
[12] S. Rangan, J.-J. Gallet, F. Bournel, S. Kubsky, K. Le Guen, G. Dufour, F. Rochet, F. Sirotti, S. Carniato, and V. Ilakovac, Phys. Rev. B **71**, 165318 (2005).
[13] F. Bournel, S. Carniato, G. Dufour, J.-J. Gallet, V. Ilakovac, S. Rangan, F. Rochet, and F. Sirotti, Phys. Rev. B **73**, 125345 (2006).
[14] T. R. Leftwich and A. V. Teplyakov, Surf. Sci. Rep. **63**, 1 (2008).
[15] F. Halverson, R. F. Stamm, and J. J. Whalen, J. Chem. Phys. **16**, 808 (1948).
[16] F. Motte-Tollet, D. Messina, and M.-J. Hubin-Franskin, J. Chem. Phys. **103**, 80 (1995).
[17] V. Ilakovac, S. Carniato, J.-J. Gallet, E. Kukk, D. Horvatić, and A. Ilakovac, Phys. Rev. A **77**, 012516 (2008).
[18] A. D. Becke, J. Chem. Phys. **98**, 5648 (1993).
[19] C. Lee, W. Yang, and R. G. Parr, Phys. Rev. **38**, 3098 (1988).
[20] M. W. Schmidt *et al.*, J. Comput. Chem. **14**, 1347 (1993).
[21] W. Kutzelnig, U. Fleisher, and M. Schindler, *The* IGLOO-*Method: Ab Initio Calculations and Interpretation of NMR Chemical Shifts and Magnetic Susceptibilities*, Vol. 23 (Springer-Verlag, Heidelberg, 1990).
[22] R. Krishnan, J. S. Binkley, R. Seeger, and J. A. Pople, J. Chem. Phys. **72**, 650 (1980).
[23] L. Triguero, O. Plashkevych, L. G. M. Petersson, and H. Ågren, J. Electron Spetrosc. Relat. Phenom. **104**, 195 (1999).
[24] T. Ziegler, A. Rauk, and E. J. Baerends, Theor. Chim. Acta **43**, 261 (1977).
[25] K. H. Hellwege and A. M. Hellwege, eds., *Landolt-Bornstein: group II: Atomic and Molecular Physics Volume 7: Structure Data of Free Polytomic Molecules* (Springer-Verlag, Berlin, 1976).
[26] D. R. Lide, ed., *Handbook of Chemistry and Physics*, 74th ed. (CRC Press, Boca Raton, 1993).
[27] M. Raynaud, J. Riga, C. Raynaud, and Y. Ellinger, J. Electron Spetrosc. Relat. Phenom. **53**, 251 (1991).
[28] M.-J. Hubin-Franskin, H. Aouni, D. Duflot, F. Motte-Tollet, C. Hannay, L. F. Ferreira, and G. Tourillon, J. Chem. Phys. **106**, 35 (1997).
[29] Ph. Parent, C. Laffon, G. Tourillon, and A. Cassuto, J. Phys. Chem. **99**, 5058 (1995).
[30] C. Kolczewski, R. Püttner, O. Plashkevych, H. Ågren, V. Staemmler, M. Martins, G. Snell, S. Schlachter, M. Sant'Anna, G. Kaindl, and L. G. M. Pettersson, J. Chem. Phys. **115**, 6426 (2001).